Elastic properties of multi-cracked composite materials

S. Giordano, M.I. Saba and L. Colombo

Regular Article

Elastic properties of multi-cracked composite materials

S. Giordano[a], M.I. Saba, and L. Colombo

Department of Physics of the University of Cagliari and Istituto Officina dei Materiali del CNR (CNR-IOM) Unità SLACS, Cittadella Universitaria, 09042 Monserrato (Ca), Italy

Abstract. The problem of predicting the effective elastic properties of multi-cracked and/or composite materials is both fundamental in materials mechanics and of large technological impact. In this paper we develop a continuum elasticity model, based on the Eshelby theory and on the differential homogenization technique, for the effective elastic moduli of a fibro-reinforced system and we address it to elaborate an estimation of the average failure condition of such composites.

1 Introduction

This work is aimed at evaluating the effective elastic properties of materials containing a given distribution of cracks and inclusions. A paradigmatic example of such multi-cracked materials with large technological impact is offered by nanocomposites (i.e. nanofibro-reinforced materials): here a tailored texture of fibers is inserted into a matrix, so generating a structure with overall improved mechanical properties (e.g., higher fracture toughness) [1,2]. In many real applications carbon nanotubes and nanofibers (also chemically functionalized) are used in reinforced composites [3,4]. Moreover, silicon carbide composites reinforced by carbon fibers (C/SiC) are ceramic materials, characterized by thermo-mechanical stability, low density and high fracture toughness [5,6].

While the overall effect of a crack population embedded in a homogeneous matrix has been evaluated by the method of tractions (or pseudotractions) [7,8], through the self-consistent technique [9] and by the differential methodology [10–12], the interplay among cracks and reinforcing inclusions (like, e.g., fibers) is still largely unexplored. In the present paper we introduce a methodology for homogenizing a multi-cracked and composite material, taking into account the interactions between cracks and reinforcing particles. This work, therefore, belongs to the vast field of homogenization techniques [13,14].

As for the elastic characterisation of dispersions, several works have been developed: an exact result exists for a material composed by a very dilute concentration of spherical or cylindrical inclusions dispersed in a solid matrix. This result, attributed to several authors [15,16], has been generalized to the case of any finite volume fraction by iterative [17,18] or differential [19–21] methods both for spherical or cylindrical inclusions [22] and for ellipsoidal particles [23].

From the historical point of view, one of the first attempt to obtain the effective behavior of an elastic dispersion has been performed through a self-consistent method (SCM) leading to the so-called Mori-Tanaka scheme [24]. The range of validity of such a method has been discussed for a polydisperse (size) suspension of spherical inclusions in a continuous matrix phase [25]. Moreover, specific results have been obtained for composites reinforced by aligned or randomly oriented, transversely isotropic fibers or platelets by using the above Mori-Tanaka scheme [26]. A further generalization has been performed through a method to obtain the transversely-isotropic effective thermomechanical properties of unidirectional composites reinforced with arbitrarily coated cylindrical fibers [27]. Some other methodologies have been developed as well to cope with different phases forming the reinforcing system: for example, the double-inclusion model (formed by an ellipsoidal inclusion with an ellipsoidal heterogeneity, embedded in an infinitely extended homogeneous domain) has been introduced and it has been generalized to the multi-inclusion model [28]. These approaches have been applied to a composite containing inclusions with multilayer coatings and to a composite consisting of several distinct materials: in each case their overall moduli are analytically estimated [28]. Finally, a generalized self-consistent method (GSCM) based on the energy equivalence and a matrix-composite model have been proposed and broadly applied to composites with three or more phases [29].

The above theoretical methods have a common feature, namely: they have been applied to single- or multiple-phase reinforcing inclusions, but do not take into consideration the interplay among inclusions and cracks. Therefore, we devote the first part of the present paper to the development of a differential method which is able to consider (arbitrarily large) volume fractions of an arbitrary number of interacting populations of different inhomogeneities (either reinforcing inclusions or cracks)

a e-mail: stefano.giordano@dsf.unica.it
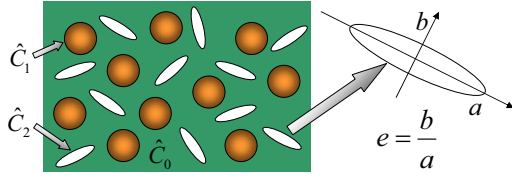
Fig. 1. (Color online) Scheme of a multicracked and fibro-reinforced material. $\hat{C}_0$, $\hat{C}_1$ and $\hat{C}_2$ are, respectively, the stiffness tensors of the matrix, the cracks and the inclusions. On the right we sketch the geometrical parameters for the elliptic cracks.

embedded in the hosting matrix. In particular, we derive a set of ordinary differential equations describing the effective elastic moduli (the stiffness tensor) of the composite structure with an arbitrary stoichiometric composition.

In the second part of the present paper we investigate the paradigmatic situation of a fibro-reinforced and multi-cracked composite material with parallel cylindrical fibers, much stiffer than the host matrix. In this case fibres and cracks represent two different embedded populations. A schematic representation of such a structure can be found in Figure 1, where the geometric details are shown. This situation ideally meets the C/SiC case above discussed. The present differential method is addressed to obtain the effective elastic behavior of this system through a pair of closed-form relationships (for the effective Young modulus and the Poisson ratio, respectively). The resulting elastic model is discussed with the support of numerical results, which describe the behavior of the system with different properties of its constituents.

Finally, we describe an approximate application of the Griffith stability criterion for a composite material, degraded by a given assembly of cracks. We obtain an estimation of the average failure stress in terms of the volume fraction of reinforcing fibres and the crack density. It is therefore possible to predict approximately the actual volume fraction of fibers to embed in order to get the desired value of failure stress, when it is defined the largest crack density admitted in the sample.

The structure of the paper is the following: in Section 2 we outline the multicomponent differential procedure. In Section 3 we describe the application of such a method to the multi-cracked and fibro-reinforced structure. Finally, in Section 4 we describe the estimation of the failure stress for the heterogeneous system.

2 Multicomponent differential method

In general, we define a composite as a matrix (with stiffness tensor $\hat{C}_0$) embedding N populations of different inclusions, characterized by volume fractions v_i and stiffness tensors $\hat{C}_i$ ($i = 1...N$). For isotropic phases each stiffness tensors $\hat{C}_i$ can be written in terms of the Young modulus E_i and the Poisson ratio ν_i, taking into account the elastic response of the i-th material [30–32]. As customary in micromechanics [33–35], we assume that each inclusion is an ellipsoid, since such a shape is the mother geometry of

all the structures of interest for this work (i.e., cylindrical fibers and slit cracks). For sake of simplicity, all the ellipsoids of the i-th population are taken equal. Within this framework, we make use of the Eshelby theory [36,37] for describing their elastic behavior upon loading. This theory provides the relationship between the uniform strain $\hat{\epsilon}_i$ within each inclusion and the remotely applied strain $\hat{\epsilon}_0$, namely: $\hat{\epsilon}_i = \left[\hat{I} - \hat{S}_i \left(\hat{I} - \hat{C}_0^{-1}\hat{C}_i \right) \right]^{-1} \hat{\epsilon}_0$, where $\hat{S}_i$ is the Eshelby tensor of the i-th population [33]. In the case of randomly oriented inclusions, we are interested in the average value $\langle \hat{\epsilon}_i \rangle = \hat{A}_i \hat{\epsilon}_0$ of the internal strain over all the possible orientations of the ellipsoids, where we have defined $\hat{A}_i = \langle \left[\hat{I} - \hat{S}_i \left(\hat{I} - \hat{C}_0^{-1}\hat{C}_i \right) \right]^{-1} \rangle$ [23].

The application of the Eshelby theory leads to a first homogenization step valid only for diluted dispersions. Under the assumption $v_i \ll 1$, we can evaluate the average strain in the system as

$$\langle \hat{\epsilon} \rangle = \left(1 - \sum_i v_i \right) \hat{\epsilon}_0 + \sum_i v_i \langle \hat{\epsilon}_i \rangle. \tag{1}$$

On the other hand, the average value of the stress tensor is given by

$$
\begin{aligned}
\langle \hat{T} \rangle &= \frac{1}{V} \int_V \hat{T} dv \\
&= \frac{1}{V} \int_{V_0} \hat{T} dv + \frac{1}{V} \sum_i \int_{V_i} \hat{T} dv \\
&= \frac{1}{V} \hat{C}_0 \int_{V_0} \hat{\epsilon} dv + \frac{1}{V} \sum_i \hat{C}_i \int_{V_i} \hat{\epsilon} dv \\
&\quad + \frac{1}{V} \hat{C}_0 \sum_i \int_{V_i} \hat{\epsilon} dv - \frac{1}{V} \hat{C}_0 \sum_i \int_{V_i} \hat{\epsilon} dv \\
&= \frac{1}{V} \hat{C}_0 \int_V \hat{\epsilon} dv + \sum_i \frac{V_i}{V} (\hat{C}_i - \hat{C}_0) \frac{1}{V_i} \int_{V_i} \hat{\epsilon} dv \\
&= \hat{C}_0 \langle \hat{\epsilon} \rangle + \sum_i v_i (\hat{C}_i - \hat{C}_0) \langle \hat{\epsilon}_i \rangle \tag{2}
\end{aligned}
$$

where V_0 is the volume of the matrix, V_i is the volume of the i-th population of inclusions and V is the total volume of the composite material. By drawing a comparison between the expressions for $\langle \hat{\epsilon} \rangle$ and $\langle \hat{T} \rangle$, we eventually obtain the effective stiffness tensor

$$
\begin{aligned}
\hat{C}_{eff} &= \hat{C}_0 + \sum_i v_i (\hat{C}_i - \hat{C}_0) \hat{A}_i \\
&\quad \times \left[\left(1 - \sum_i v_i \right) \hat{I} + \sum_i v_i \hat{A}_i \right]^{-1}. \tag{3}
\end{aligned}
$$

In the present case of diluted dispersions with $v_i \ll 1$ equation (3) can be simplified by neglecting the last inverse tensor [38]. Therefore, the final expression for the effective stiffness tensor is

$$\hat{C}_{eff} = \hat{C}_0 + \sum_i v_i (\hat{C}_i - \hat{C}_0) \hat{A}_i. \tag{4}$$

For brevity, equation (4) can be summarized in the form $\hat{C}_{eff} = f(\hat{C}_0, \{\hat{C}_i\}, \{v_i\})$, where the function f fully describes the effective behavior of a dilute dispersion.

The next step is to consider higher values of the volume fractions. We define V_i as the volume of the i-th population of inclusions and V as the total volume of the composite material (so that $v_i = \frac{V_i}{V}$). An iterative scheme can be implemented by using a single scalar variable t defined by $v_i = \alpha_i t$, with $\sum_i \alpha_i = 1$ and $0 \le t \le 1$. We observe that t represents the total volume fraction of inclusions since $\sum_i v_i = \sum_i \alpha_i t = t$. We consider the initial configuration with $v_i = \frac{V_i}{V} = \alpha_i t$ and $V_i = \alpha_i t V$, for a very small t. The initial effective elastic tensor is calculated as $\hat{C}_{eff} = f(\hat{C}_0, \{\hat{C}_i\}, v_i)$, according to equation (4).

Next, we slightly increase the inclusions volume by $\Delta V_i = \alpha_i \Delta t V$ and we get the corresponding effective stiffness tensor $\hat{C}'_{eff} = f(\hat{C}_{eff}, \{\hat{C}_i\}, v'_i)$. We stress that

$$v'_i = \frac{\Delta V_i}{V + \sum_k \Delta V_k} = \frac{\Delta t}{1 + \Delta t} \alpha_i \qquad (5)$$

are the volume fractions of the inclusions embedded in a virtual matrix of stiffness tensor $\hat{C}_{eff}$. Since Δt is small by construction, it is possible to elaborate a first order expansion of $\hat{C}'_{eff}$

$$\hat{C}'_{eff} = \hat{C}_{eff} + \sum_i \frac{\partial f^*}{\partial v_i} \frac{\Delta t}{1 + \Delta t} \alpha_i, \qquad (6)$$

where the symbol $*$ means that $\frac{\partial f^*}{\partial v_i}$ must be calculated for $v_i = 0$ and $\hat{C}_0 = \hat{C}_{eff}$. Through the above procedure we can identify the initial volume fractions $v_i^{in} = \alpha_i t$ and the actual final volume fractions

$$v_i^{fin} = \frac{V_i + \Delta V_i}{V + \sum_k \Delta V_k} = \alpha_i \frac{t + \Delta t}{1 + \Delta t}. \qquad (7)$$

Therefore, the corresponding increments are given by

$$\Delta v_i = v_i^{fin} - v_i^{in} = \alpha_i \Delta t \frac{1 - t}{1 + \Delta t}. \qquad (8)$$

We can recast equation (6) in the form

$$\hat{C}'_{eff}\left(\{v_i^{fin}\}\right) - \hat{C}_{eff}\left(\{v_i^{in}\}\right) = \sum_i \frac{\partial f^*}{\partial v_i} \frac{\Delta t}{1 + \Delta t} \alpha_i. \quad (9)$$

The increment of the variable t, when we increase the volume fractions v_i^{in} up to the values v_i^{fin}, is given by $\frac{\Delta v_i}{\alpha_i} = \Delta t \frac{1-t}{1+\Delta t}$. So, by dividing both sides of equation (9) by the quantity $\frac{\Delta v_i}{\alpha_i} = \Delta t \frac{1-t}{1+\Delta t}$, we obtain the differential quotient of the effective elastic tensor $\hat{C}_{eff}$. Finally, in the limit of $\Delta t \to 0$, the iterative scheme converges to a differential equation

$$\frac{d\hat{C}_{eff}}{dt} = \frac{1}{1-t} \sum_i \frac{\partial f^*}{\partial v_i} \alpha_i \qquad (10)$$

with initial condition $\hat{C}_{eff}(t = 0) = \hat{C}_0$. Once solved the differential equation, we must restore t and α_i through the identities $t = \sum_i v_i$ and $\alpha_i = v_i / \sum_k v_k$.

3 Effective behavior of the multi-cracked composite

We now address the above formal device to the paradigmatic heterogeneous system we are going to investigate. We consider an isotropic matrix with an elastic tensor $\hat{C}_0$ embedding just two kinds of inclusions, namely: an assembly of rigid parallel cylindrical fibers (stiffness $\hat{C}_1$ with Young modulus $E_1 \to \infty$) and an assembly of slit cracks (stiffness $\hat{C}_2$ with $E_2 \to 0$). The corresponding volume fractions are v_1 and v_2, respectively. All the inclusions are oriented along the same direction perpendicular to a given plane, as shown in Figure 1. We impose the plane strain condition, thus translating our problem into a two-dimensional one. We remark that the slit cracks are randomly oriented within the plane and, therefore, we will observe an overall isotropic elastic behavior of the two-dimensional system [10].

Provisionally, a slit crack is treated as a cylinder with a strongly oblate elliptic base (corresponding to a vanishing aspect ratio e, as defined in Fig. 1). This approach is very convenient since we will develop our arguments by taking profit from general results holding for ellipsoidal inclusions [33,34]. Since the area of the elliptic base is given by $\pi ab = \pi e a^2$ (see Fig. 1), we can easily obtain the volume fraction of the assembly of cracks as $v_2 = N\pi e a^2 / A = \phi e$, where N is the number of cracks dispersed over the area A and $\phi = N\pi a^2 / A$ is the crack density. From now on, the two variables $v_1 = c$ (volume fraction of fibers) and ϕ (crack density) will be used to describe the composition of the system.

We can combine the general result given in equation (4) with the specific case of dilute populations of fibers and cracks. In both cases, we benefit of the explicit expressions for the Eshelby tensors, hereafter referred to as $\hat{S}_1$ and $\hat{S}_2$, respectively [33]. In the present case equation (4), taking into account the population of random oriented elliptic cylinders (void) and the population of reinforcing circular cylinders (rigid), assumes the form

$$\hat{C}_{eff} = \hat{C}_0 + v_1(\hat{C}_1 - \hat{C}_0)\hat{A}_1 - v_2\hat{C}_0\hat{A}_2 \qquad (11)$$

where for the reinforcing fibres we have $v_1 = c$ and

$$\hat{A}_1 = \left[\hat{I} - \hat{S}_1(\hat{I} - \hat{C}_0^{-1}\hat{C}_1)\right]^{-1} \qquad (12)$$

and for the random oriented cracks $v_2 = \phi e$ and

$$\hat{A}_2 = \langle(\hat{I} - \hat{S}_2)^{-1}\rangle. \qquad (13)$$

After some algebra concerning the limiting value of $\hat{C}_{eff}$ for $E_1 \to \infty$, the homogenization procedure eventually provides the effective Young modulus E_{eff} and the effective Poisson ratio E_{eff}

$$E_{eff} = E_0(1 + c\mathcal{G}_c + \phi e\mathcal{G}_\phi)$$
$$E_{eff} = \nu_0 + c\mathcal{H}_c + \phi e\mathcal{H}_\phi \qquad (14)$$

where we have introduced the four quantities $\mathcal{G}_c$, $\mathcal{G}_\phi$, $\mathcal{H}_c$ and $\mathcal{H}_\phi$ as follows

$$\mathcal{G}_c = \frac{(\nu_0 - 1)(8\nu_0^2 - 2\nu_0 + 5)}{(4\nu_0 - 3)(\nu_0 + 1)}$$

$$r\mathcal{G}_\phi = \frac{(\nu_0 - 1)(2\nu_0 e^2 + 2\nu_0 + 4\nu_0 e + e^2 + e + 1)}{e(\nu_0 + 1)}$$

$$\mathcal{H}_c = \frac{(\nu_0 - 1)(2\nu_0 - 1)(4\nu_0 - 1)}{4\nu_0 - 3}$$

$$\mathcal{H}_\phi = \frac{e - 3\nu_0 e + 2\nu_0^2 e - \nu_0 + \nu_0^2 - \nu_0 e^2 + e^2 \nu_0^2}{e}. \quad (15)$$

The slit crack geometry is finally recovered through the limit $b \to 0$ or, equivalently, $e \to 0$. We get

$$E_{eff} = E_0 + cE_0 \frac{(\nu_0 - 1)(8\nu_0^2 - 2\nu_0 + 5)}{(4\nu_0 - 3)(\nu_0 + 1)}$$

$$+ \phi E_0 \frac{(\nu_0 - 1)(2\nu_0 + 1)}{\nu_0 + 1}$$

$$\nu_{eff} = \nu_0 + c\frac{(\nu_0 - 1)(2\nu_0 - 1)(4\nu_0 - 1)}{4\nu_0 - 3}$$

$$+ \phi\nu_0(\nu_0 - 1). \quad (16)$$

While equation (16) is valid in the dilute limit, we aim at applying the above differential scheme in order to cope with arbitrarily large volume fractions of fibers and cracks. This can be done by using equation (10), where $\frac{\partial f^*}{\partial v_i}$ may be easily obtained from equations (15) and (16). The resulting system of differential equations for the effective elastic moduli is

$$\frac{dE_{eff}}{dt} = \frac{1}{1-t} \left(\alpha_1 \mathcal{G}_c + \alpha_2 \mathcal{G}_\phi \right) E_{eff}$$

$$\frac{d\nu_{eff}}{dt} = \frac{1}{1-t} \left(\alpha_1 \mathcal{H}_c + \alpha_2 \mathcal{H}_\phi \right), \quad (17)$$

where the functions $\mathcal{G}_c, \mathcal{G}_\phi, \mathcal{H}_c$ and $\mathcal{H}_\phi$ must be evaluated for $\nu_0 = \nu_{eff}$. Of course, we consider the initial conditions $E_{eff}(t = 0) = E_0$ and $\nu_{eff}(t = 0) = \nu_0$. The problem can be solved through a couple of integrations as follows

$$\int_{\nu_0}^{\nu_{eff}} \frac{\alpha_1 \mathcal{G}_c(\nu_{eff}) + \alpha_2 \mathcal{G}_\phi(\nu_{eff})}{\alpha_1 \mathcal{H}_c(\nu_{eff}) + \alpha_2 \mathcal{H}_\phi(\nu_{eff})} d\nu_{eff} = \int_{E_0}^{E_{eff}} \frac{dE_{eff}}{E_{eff}}$$

$$\int_{\nu_0}^{\nu_{eff}} \frac{d\nu_{eff}}{\alpha_1 \mathcal{H}_c(\nu_{eff}) + \alpha_2 \mathcal{H}_\phi(\nu_{eff})} = \int_0^t \frac{dt}{1-t}. \quad (18)$$

Once performed the integrations, the relations $t = c + \phi e$, $\alpha_1 = \frac{c}{c + \phi e}$ and $\alpha_2 = \frac{\phi e}{c + \phi e}$ are used in order to eliminate the temporary parameters t, α_1 and α_2 and to introduce the real quantities c and ϕ. Finally, by taking the limit of $e \to 0$, we obtain the key result of the present investigation for a multi-cracked composite, namely an implicit equation for the effective Poisson ratio

$$\ln \frac{1 - \nu_{eff}}{1 - \nu_0} + \ln \left[(1-c)^{3 + \frac{\phi}{c}} \right] + \frac{s}{2} - \frac{14c + 3\phi}{2c + \phi} \frac{r}{2q} = 0 \quad (19)$$

and the explicit form of the effective Young modulus

$$\ln \frac{E_{eff}}{E_0} = -\frac{\phi}{2c + \phi} \frac{s}{2} - \ln \frac{1 + \nu_0}{1 + \nu_{eff}} - \frac{8c - 3\phi}{2c + \phi} \frac{r}{2q}, \quad (20)$$

where we have defined the parameters

$$q = \sqrt{\frac{2c + 9\phi}{2c + \phi}}$$

$$r = \ln \left[\frac{q + 3 - 8\nu_0}{q + 3 - 8\nu_{eff}} \frac{q - 3 + 8\nu_{eff}}{q - 3 + 8\nu_0} \right]$$

$$s = \ln \left[\frac{c + \nu_0 (4\nu_0 - 3)(2c + \phi)}{c + \nu_{eff}(4\nu_{eff} - 3)(2c + \phi)} \right]. \quad (21)$$

We remark that the general result provided by equations (19) and (20) recovers the more specific case obtained in reference [10] for a multi-cracked homogeneous material (i.e., for $c = 0$). The same also holds for the particular case of a purely fibrous material ($\phi = 0$): present findings are consistent with previous literature [22]. More specifically, if we consider $c = 0$ we obtain the explicit expressions

$$\nu_{eff} = \frac{\nu_0}{\nu_0 + (1 - \nu_0)e^\phi} \quad (22)$$

$$E_{eff} = E_0 \frac{2\nu_0 + (1 - \nu_0)e^\phi}{[\nu_0 + (1 - \nu_0)e^\phi]^2(1 + \nu_0)}. \quad (23)$$

In this case the relation giving the effective Poisson ratio has been explicitly solved as shown in equation (22). Then, it is used in the relation for E_{eff} by obtaining equation (23). On the other hand, when $\phi = 0$ (purely fibrous material) we eventually obtain

$$\left(\frac{1 - \nu_{eff}}{1 - \nu_0} \right)^{1/3} \frac{2\nu_{eff} - 1}{2\nu_0 - 1} \left(\frac{1 - 4\nu_0}{1 - 4\nu_{eff}} \right)^{4/3} (1 - c) = 1 \quad (24)$$

$$E_{eff} = E_0 \frac{1 + \nu_{eff}}{1 + \nu_0} \left(\frac{1 - 2\nu_{eff}}{1 - 2\nu_0} \right)^2 \left(\frac{1 - 4\nu_0}{1 - 4\nu_{eff}} \right)^2. \quad (25)$$

In this case equation (24) giving the effective Poisson ratio can not be solved explicitly and it remains in implicit form.

With the aim of analyzing the behavior of E_{eff} and ν_{eff} described by equations (19) and (20) we show a series of numerical results obtained for different values of the matrix Poisson ratio. The results are organized as follows: $\nu_0 = -0.8$ in Figure 2; $\nu_0 = -0.5$ in Figure 3; $\nu_0 = 0.25$ in Figure 4 and, finally, $\nu_0 = 0.4$ in Figure 5. The first two cases concern a negative Poisson ratio of the matrix, corresponding to the realistic cases reported for foams [39]. The other two cases show the results for positive values of the matrix Poisson ratio, typical of brittle and ceramic materials.

In Figure 2 (right) we note that when $c \to 0$ and $\phi \to 0$ we obtain $\nu_{eff} \to \nu_0$, as expected for a matrix without any inclusion (fiber or crack). Moreover, Figure 2 (right) shows that, for $\phi = 0$ and $c \to 1$ (i.e. without cracks), we obtain $\nu_{eff} \to 1/4$. This property can, in fact, be easily verified by equation (24), and it is satisfied for any value of ν_0.
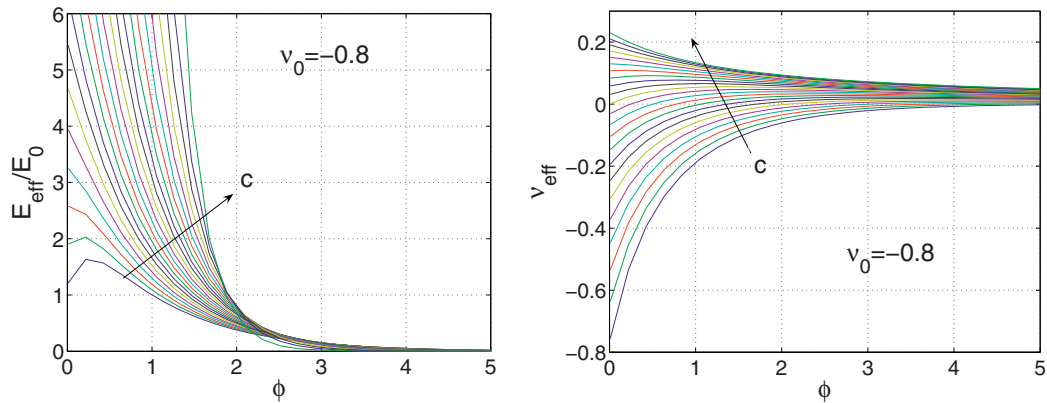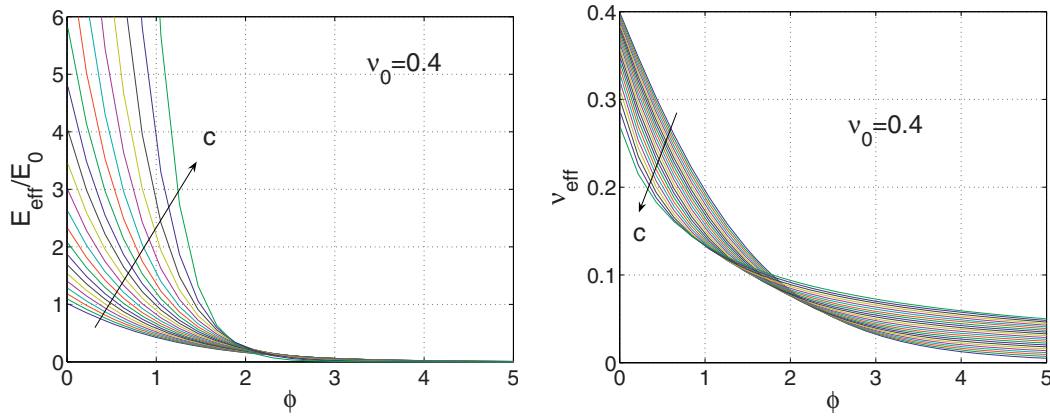
Fig. 2. (Color online) Effective Young modulus E_{eff} (left) and effective Poisson ratio ν_{eff} (right) in terms the crack density ϕ calculated for a matrix with $\nu_0 = -0.8$. The arrow marked by c indicates an increasing volume fraction of fibers in the range $0 < c < 1$. E_{eff} is normalized to the value E_0 of the matrix Young modulus.
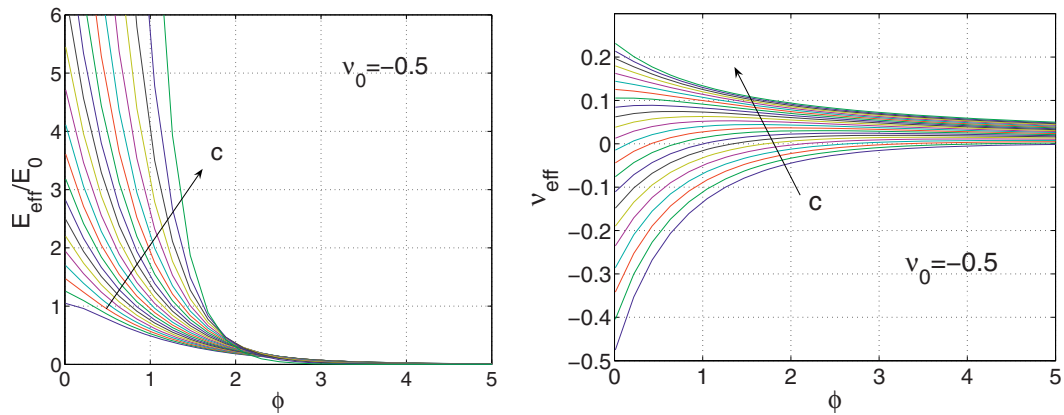
Fig. 3. (Color online) Effective Young modulus E_{eff} (left) and effective Poisson ratio ν_{eff} (right) in terms the crack density ϕ calculated for a matrix with $\nu_0 = -0.5$. The arrow marked by c indicates an increasing volume fraction of fibers in the range $0 < c < 1$. E_{eff} is normalized to the value E_0 of the matrix Young modulus.
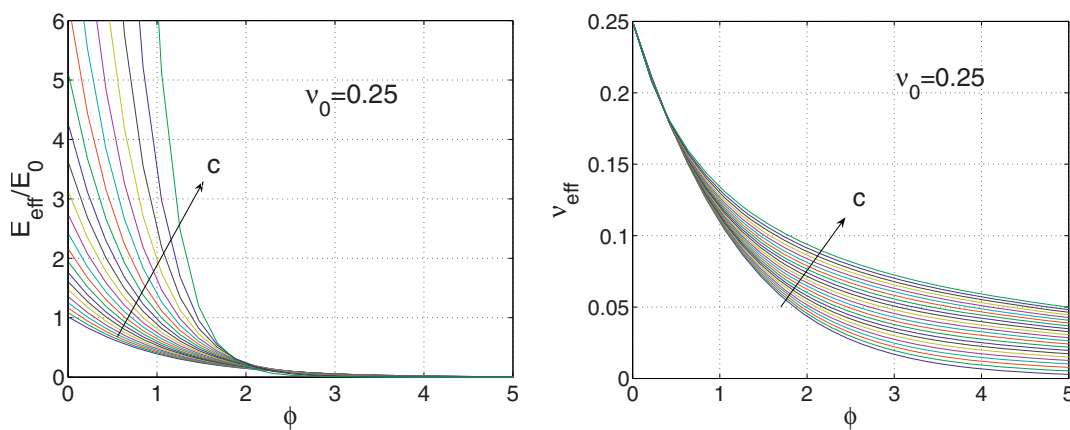
Fig. 4. (Color online) Effective Young modulus E_{eff} (left) and effective Poisson ratio ν_{eff} (right) in terms the crack density ϕ calculated for a matrix with $\nu_0 = 0.25$. The arrow marked by c indicates an increasing volume fraction of fibers in the range $0 < c < 1$. E_{eff} is normalized to the value E_0 of the matrix Young modulus.

Fig. 5. (Color online) Effective Young modulus E_{eff} (left) and effective Poisson ratio ν_{eff} (right) in terms the crack density ϕ calculated for a matrix with $\nu_0 = 0.4$. The arrow marked by c indicates an increasing volume fraction of fibers in the range $0 < c < 1$. E_{eff} is normalized to the value E_0 of the matrix Young modulus.

We also observe that the value of the Poisson ratio tends to become positive for both increasing values of c and ϕ. This phenomenon can be explained by observing that the extreme cases of void material and rigid material have an elastic behavior which is in opposition to the elastic response defined by a negative Poisson ratio (where a given traction leads to a dilatation in the transverse directions).

As for the effective Young modulus shown in Figure 2 (left), we obtain, for low values of ϕ and c, a value greater than the Young modulus of the original elastic matrix. This is an interesting unconventional behavior of the effective Young modulus of the multicracked composite solid, exhibited for negative Poisson ratio of the matrix. It can be explained as follows: to begin, we consider the simpler case with $c = 0$ (without fibres). The derivative of equation (23) with respect to ϕ (evaluated for $\phi = 0$) can be simply obtained as

$$\frac{dE_{eff}}{d\phi}|_{\phi=0} = E_0 \frac{(\nu_0 - 1)(1 + 2\nu_0)}{\nu_0 + 1}. \tag{26}$$

Therefore, the curve E_{eff}/E_0 versus ϕ shows a maximum for $-1 < \nu_0 < -1/2$. Accordingly, equation (26) is positive for $-1 < \nu_0 < -1/2$ proving that the effective Young modulus is an increasing function of ϕ around the point $\phi = 0$. This phenomenon remains observable for low values of the fibre volume fraction c and disappears for higher values of c. Evidently, for values of ϕ after the maximum, the effective Young modulus is definitively decreasing, describing the progressive degradation of the multi-cracked material. Moreover, the curves for E_{eff}/E_0 in Figure 2 (left) show the reinforcing effects of the fibres embedded in the composite material: the exponential increase of E_{eff}/E_0 with c is in fact evident.

In the case with $\nu_0 = -1/2$, the curves of ν_{eff} shown in Figure 3 (right) do not exhibit important variation with respect to the previous case with $\nu_0 = -0.8$. On the contrary, as for the effective Young modulus, it is important to note that the value $\nu_0 = -1/2$ represents a transition in the elastic behavior. As a matter of fact, as shown in equation (26), for $\nu_0 = -1/2$ we have $\frac{dE_{eff}}{d\phi}|_{\phi=0} = 0$. It

means that, for $\phi \to 0$ and $c = 0$, the curve of E_{eff}/E_0 approaches the value 1 with horizontal tangent line, as clearly shown in Figure 3 (left).

We consider now the first case with a positive Poisson ratio $\nu_0 = 0.25$. Figure 4 (right) shows that $\nu_{eff} = 1/4$ for $\phi = 0$ and for any value of the volume fraction c of fibres. This behavior is in perfect agreement with the above stated property: without cracks ($\phi = 0$) and with an high concentration of fibres ($c \to 1$) we have $\nu_{eff} \to 1/4$. In other words, we can say that the value $\nu_0 = 1/4$ assumes the role of a fixed point for the Poisson ratio of the fibrous material. As for the effective Young modulus, we observe in Figure 4 (left) a qualitative behavior similar to the previous results. Interestingly enough, we remark that E_{eff}/E_0 decreases with ϕ starting with an initial negative slope (since $\nu_0 > -1/2$; see Eq. (26)).

Finally, we consider the case with $\nu_0 = 0.4$. We observe in Figure 5 (right) a decreasing trend of ν_{eff} (from $\nu_{eff} = 0.4$ to $\nu_{eff} = 0.25$) for $\phi = 0$ when c varies from 0 to 1. This behavior is again in perfect agreement with the property above discussed. The behavior of the effective Young modulus shown in Figure 5 (left) confirms the reinforcing effect of the distribution of cylindrical fibres in the material.

4 Failure properties

The cornerstone of linear elastic fracture mechanics for homogeneous materials is represented by the renowed Griffith criterion for brittle failure, namely [40]: upon loading, a single (isolated) slit crack propagates (i.e. the material fails) provided that the tensile load is greater than the Griffith failure stress σ_f^G. The same model provides a simple and very useful relation between σ_f^G and the Young modulus E_0 and the Poisson ratio ν_0 of the material, namely

$$\sigma_f^G = \sqrt{\frac{2\gamma_s E_0}{\pi a(1 - \nu_0^2)}}, \tag{27}$$
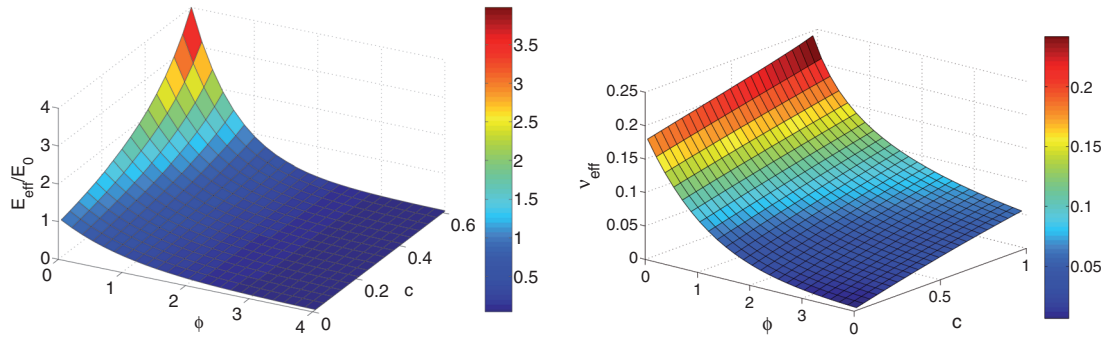
Fig. 6. (Color online) Effective Young modulus E_{eff} and effective Poisson ratio ν_{eff} in terms of the volume fraction of fibers c and the crack density ϕ calculated for a SiC matrix with $\nu_0 = 0.18$.

where we have imposed plane-strain conditions and we have indicated by a and γ_s the crack half-length and the material specific surface energy, respectively [41,42]. The Griffith criterion was originally stated in terms of an energy balance: the growth of a crack within a material under loading forces requires the creation of two new surfaces. Therefore, in order to make a material to fail (i.e. in order to make the crack to increase its length), the mechanical work of the applied external forces must exceed the work necessary to create new (internal) surface.

The Griffith criterion can be also stated in terms of the Stress Intensity Factor (SIF) K_I^G: a key quantity in linear elastic fracture mechanics describing the concentration of the stress near the crack tips, caused by a remote load. For an isolated slit crack remotely loaded in mode I by a stress σ, the asymptotic form of the tensile stress near the crack tip is $K_I^G / \sqrt{2\pi r}$ (where r is the distance from the crack tip measured on the crack plane). The linear elastic theory predicts the value of K_I^G in this case [41,42]

$$K_I^G = \sigma \sqrt{\pi a}. \tag{28}$$

The Griffith criterion can be also stated by affirming that the crack propagates if $K_I^G \geq K_{I,f}^G$ where the quantity $K_{I,f}^G = \sqrt{2\gamma_s E_0/(1-\nu_0^2)}$ is the so-called fracture toughness, which a material constant.

From a conceptual point of view the energy balance underlying the Griffith criterion can be also applied to a population of cracks dispersed in a given body. Nevertheless, in such a case, the surface energy associated with the population of cracks can be simply evaluated while the elastic energy of the system under stress is not available in closed form (since the elastic fields in this complex case can not be evaluated analytically). Therefore, although the energy balance still remains the key conceptual item, it is very hard to exploit it in order to determine the failure condition. So, the Griffith theory can be explicitly applied only to an isolated crack, embedded in a homogeneous material: a situation quite far off the common practice. As a matter of fact, real materials (both manufactured and natural) contain full populations of cracks (possibly taking a large density) and display compositional fluctuations (because of elastic inclusions, defects, precipitates or fibers).

While the effective Youngs modulus and the effective Poisson ratio are volume averaged quantities and they are almost insensitive to clustering of the inhomogeneities or specific spatial distributions of the inclusions, the failure stress and the stress intensity factor are very sensitive to the mutual positions of inhomogeneities. This is true since their definitions depend on the worst case of spatial arrangement of cracks and fibres. From this point of view, these quantities can not be determined by an homogenization technique, as the present one. Nevertheless, we can obtain a rough estimate of the failure stress and the stress intensity factor by supposing a uniform or regular distribution of objects within the matrix. It means that we are evaluating the average value of a random variable which is, however, characterized by a large value of the standard deviation.

We can use equations (19) and (20) for analyzing the fracture mechanics of a multi-cracked and fibro-reinforced material. An application of these results is given in Figure 6 where E_{eff} and ν_{eff} are shown for a SiC matrix ($\nu_0 = 0.18$). By considering a random distribution of fibers and cracks as shown in Figure 1, the effective average failure stress σ_f^{eff} in such a composite system can be straightforwardly obtained from equation (27) by replacing ν_0 and E_0 with ν_{eff} and E_{eff}. It means that we are calculating the average value of failure stress over all the possible configurations with given volume fraction of fibres and cracks. Therefore, σ_f^{eff} is simply provided by the following relation

$$\sigma_f^{eff} = \sigma_f^G \sqrt{\frac{E_{eff}}{E_0} \frac{1-\nu_0^2}{1-\nu_{eff}^2}}. \tag{29}$$

The estimate in equation (29) reflects how failure properties are affected by the presence of heterogeneities. Therefore, it can be used also as rough estimate of the changes of the intrinsic toughness induced by the presence of the heterogeneities. It is important to observe that there are two specific cases where the estimate given in equation (29) should be assumed as a good approximation of the real failure stress: (i) when the cracks and the reinforcing fibres are uniformly spaced (in average sense) in the space (in this case all the effects induced by the proximity of the heterogeneities are avoided); (ii) when we are
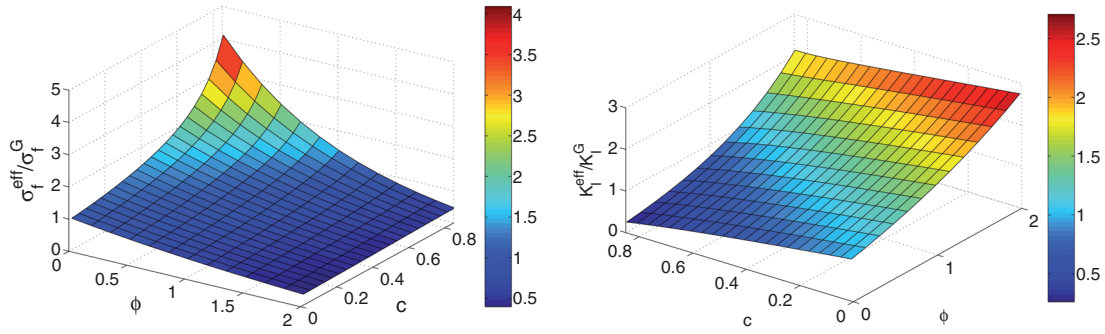
Fig. 7. (Color online) Effective failure stress σ_f^{eff} (left) and stress intensity factor K_I^{eff} (right) for a multi-cracked composite as function of fiber and crack density. Both quantities are normalized to the corresponding value for an homogeneous matrix containing just a crack.
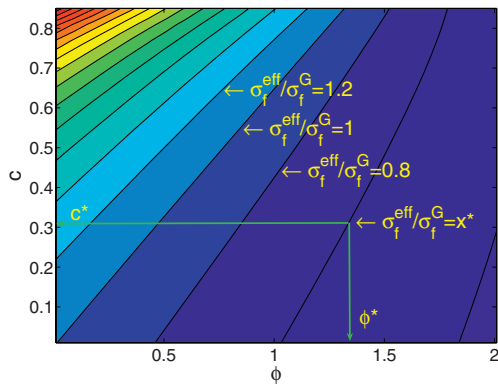
Fig. 8. (Color online) Contour plot of $\sigma_f^{eff}/\sigma_f^G$ in terms of the volume fraction of fibers c and the crack density ϕ.

dealing with cracks with the length much greater than the radius of the fibres and small ϕ (in this case the population of cracks can be considered quite exactly as embedded in an effective homogeneous matrix).

In Figure 7 (left) we show the $\sigma_f^{eff}/\sigma_f^G$ ratio versus the fiber (c) and crack (ϕ) densities for the actual case of a SiC matrix. If $c = 0$ we obtained the exact exponential law $\sigma_f^{eff}/\sigma_f^G = \exp(-\phi/2)$, which explains and quantifies the degradation phenomenon with an increasing crack density. Moreover, the $\sigma_f^{eff}/\sigma_f^G$ trend versus c quantitatively predicts the reinforcing features due to the fibers.

In Figure 7 (right) we have also shown the ratio between the Stress Intensity Factor (SIF, in mode I) of a crack in the composite material and an isolated crack of the same size [41,42]. This plot has been obtained by observing that the following relation is verified

$$\frac{K_I^{eff}}{K_I^G} = \frac{\sigma_f^G}{\sigma_f^{eff}} \qquad (30)$$

with the same degree of approximation of equation (29). It means that the SIF ratio shows a behavior which is simply the reverse of that of the failure stress.

Finally, in Figure 8 we consider the contour plot of the ratio $\sigma_f^{eff}/\sigma_f^G$: by selecting a given crack density ϕ^* admitted in a sample, it is indeed possible to directly predict the

value of the suitable volume fraction c^* of fibers that must be embedded in order to get the desired value of failure stress ratio x^*. This is shown in Figure 8 where a composite SiC system containing a ϕ^* concentration of rigid carbon fibers is considered. If we need that such a composite resists up to a maximum applied stress ratio as large as x^*, we should embed as many fibers as corresponding to a volume fraction c^*.

5 Conclusions

In conclusion, a refined iterative/differential scheme has been introduced in order to evaluate the effective elastic properties of a multi-cracked and fibrous material. The interactions among reinforcing inclusions and cracks have been taken into account in order to obtain a homogenization scheme which is valid for arbitrary values of volume fraction of fibres and crack density. The results have been shown for both negative and positive values of the matrix Poisson ratio. The case of the C/SiC composite structure has been considered from the point of view of the failure stability. We have shown that this approach allows for an approximate prediction and design of the fibro-reinforcing system, as for its failure condition.

References

1. *Handbook of Materials Modeling*, edited by G.B. Olson (Springer, Amsterdam, 2005)
2. *Ceramic Armour Materials By Design*, edited by J.W. McCauley et al. (The American Ceramic Society, Westerville, Ohio, 2002)
3. J. Li, C. Papadopoulos, J.M. Xu, M. Moskovits, Appl. Phys. Lett. **75**, 367 (1999)
4. S. Wang, Z. Liang, T. Liu, B. Wang, C. Zhang, Nanotechnology **17**, 1551 (2006)

5. *Ceramic Matrix Composites: Fiber Reinforced Ceramics and their Applications*, edited by W. Krenkel (Wiley-VCH, Berlin, 2008)
6. *Ceramic-Matrix Composites*, edited by R. Warren (Blackie and Son Ltd., Glasgow, 1992)
7. M. Kachanov, Appl. Mech. Rev. **45**, 305 (1992)
8. M. Kachanov, I. Sevostianov, Int. J. Solids Struct. **42**, 309 (2005)
9. Y. Huang, K.X. Hu, A. Chandra, J. Mech. Phys. Sol. **42**, 1273 (1994)
10. S. Giordano, L. Colombo, Phys. Rev. Lett. **98**, 055503 (2007)
11. S. Giordano, L. Colombo, Eng. Frac. Mech. **74**, 1983 (2007)
12. S. Giordano, L. Colombo, Phys. Rev. B **77**, 054106 (2008)
13. L.J. Walpole, Adv. Appl. Mech. **11**, 169 (1981)
14. *Heterogeneous Media: Micromechanics Modeling Methods and Simulations*, edited by K.Z. Markov, L. Preziozi, (Birkhauser, Boston, 2000)
15. Z. Hashin, J. Appl. Mech. **50**, 481 (1983)
16. J.F. Douglas, E.J. Garboczi, Adv. Chem. Phys. **91**, 85 (1995)
17. M. Avellaneda, Comm. Pure Appl. Math. **40**, 527 (1987)
18. D. Lukkassen, J. Peetre, L.E. Persson, Appl. Math. **4**, 343 (2004)
19. D.A.G. Bruggeman, Ann. der Phys. **416**, 636 (1935)
20. D.A.G. Bruggeman, Ann. der Phys. **417**, 645 (1936)
21. D.A.G. Bruggeman, Ann. der Phys. **421**, 160 (1937)
22. R. McLaughlin, Int. J. Eng. Sci. **15**, 237 (1977)
23. S. Giordano, Eur. J. Mech. - A/Solids **22**, 885 (2003)
24. T. Mori, K. Tanaka, Acta Metallurgica **21**, 571 (1973)
25. R. Christensen, H. Schantz, J. Shapiro, J. Mech. Phys. Sol. **40**, 69 (1992)
26. T. Chen, G.J. Dvorak, Y. Benveniste, J. Appl. Mech. **59**, 539 (1992)
27. A. Dasgupta, S.M. Bhandarkar, Mech. Mater. **14**, 67 (1992)
28. M. Hori, S. Nemat-Nasser, Mech. Mater. **14**, 189 (1993)
29. Y. Huang, K.X. Hu, X. Wei, A. Chandra, J. Mech. Phys. Sol. **42**, 491 (1994)
30. L.D. Landau, E.M. Lifschitz, *Theory of Elasticity, Course of Theoretical Physics*, 3rd edn. (Butterworth Heinemann, Oxford, 1986), Vol. 7
31. A.E.H. Love, *A treatise on the mathematical theory of elasticity* (Dover Publication Inc., New York, 2002)
32. A.E. Green, W. Zerna, *Theoretical elasticity* (Oxford Press, Oxford, 1954)
33. T. Mura, *Micromechanics of defects in solids* (Kluwer Academic Publishers, Dordrecht, 1987)
34. R.J. Asaro, V.A. Lubarda, *Mechanics of solids and materials* (Cambridge University Press, Cambridge, 2006)
35. R.J. Atkin, N. Fox, *An introduction to the theory of elasticity* (Dover Publication Inc., New York, 1980)
36. J.D. Eshelby, Proc. R. Soc. London A **241**, 376 (1957)
37. J.D. Eshelby, Proc. R. Soc. London A **252**, 561 (1959)
38. R.M. Christensen, *Mechanics of composite materials* (Dover Publication Inc., New York, 2005)
39. R. Lakes, Phys. Rev. Lett. **86**, 2897 (2001)
40. A.A. Griffith, Phil. Roy. Soc. (London) A **221**, 163 (1920)
41. K.B. Broberg, *Cracks and fracture* (Academic Press, London, 1999)
42. T.L. Anderson, *Fracture Mechanics: Fundamentals and Applications* (CRC Press, London, 2004)